

# Computational study of thermally controlled polymer network disassembly via the incorporation of sterically hindered urea linkages

Jitendra Malik, Stephen J. Clarson\*

*Department of Materials Science and Engineering, University of Cincinnati, Cincinnati, OH 45221-0012, USA*

Received 12 June 2001; received in revised form 26 November 2001; accepted 26 November 2001

## Abstract

Previously, our work was focused on the experimental details of the controlled thermally decrosslinking behavior of a polymer system that contained sterically hindered urea linkages. Such systems are of interest because they introduce rework capabilities into the polymeric material. The focus of this paper is to study these controllable decrosslinking systems from a theoretical perspective. In this study, computational methods were used to study the 2-(tert-butylamino)ethyl methacrylate-isophorone diisocyanate-2-(tert-butylamino)ethyl methacrylate polymer system that has been shown to undergo controlled thermal network disassembly. The following two aspects are the focus of this investigation. First, computational methods were used to suggest other structures within this family of compounds that might also be reworkable. Based on the simulation data likely candidates are suggested and the thermal decrosslinking properties are hypothesized compared with the real system that was experimentally studied. Second, heat of reaction data was determined from simulations of the decrosslinking reactions. These data were then compared with the experimental data and a predictive model was developed to estimate the decrosslinking temperature of the polymer network when exposed to a particular severing agent. © 2002 Elsevier Science Ltd. All rights reserved.

*Keywords:* Reworkable polymer networks; Molecular disassembly; Sterically hindered urea groups

## 1. Introduction

Griffith first coined the term ‘command-destruct’ to describe the concept of reworkable materials [1]. In his original idea, Griffith envisioned epoxy systems that could be selectively degraded for efficient removal of adhesively bonded components from one another. In Griffith’s view, reworkability could be imparted into any system that incorporated a means to molecularly disassemble the polymer network. Words like reworkability, molecular disassembly and controlled decrosslinking are all terms describing systems that embody Griffith’s original concept. ‘Smart materials’ that decrosslink on command would allow removal of any number of components from one another that are embedded or bonded together by the polymer matrix. An increasingly prevalent area of reworkable systems, and the subject of much active research in current manufacturing surroundings, involves electrical/electronic components [2,3]. For single chip packages, manufacturing losses due to defective semiconductor components range up to several percent and this number increases to 30% or

even higher for multi-chip configurations depending on assembly complexity [4]. Given these percentages coupled with the high volume of chip assemblies produced (ranging from 1000 for small operations per week to 100,000 for large operations per week) huge cost savings could be realized by the development of a cheap, effective packaging material that supports rework and replacement. Furthermore, there are also environmental issues that a reworkable system addresses [5]. Currently, most thermosets are intractable, which gives them longevity in adhesive strength, making them the material of choice [2,3,6–8]. However, with increasingly tough environmental legislation, manufacturers are also held responsible for the disposal and recycling of their materials. Therefore, if a material can be designed for disassembly on a molecular scale, many of the disadvantages of crosslinked networks can be addressed without losing the positive attributes of thermosets. No one ideal method exists to impart reworkability into any polymer system, though researchers have tried a variety of approaches to date [4,9–24].

The literature on reworkable resins suggested that no one ideal rework temperature is called for but rather different applications require different temperatures. Based on this observation, we wanted to design a system that allowed

\* Corresponding author. Tel.: +1-513-556-5430; fax: +1-513-556-5007.  
E-mail address: sclarson@uceng.uc.edu (S.J. Clarson).

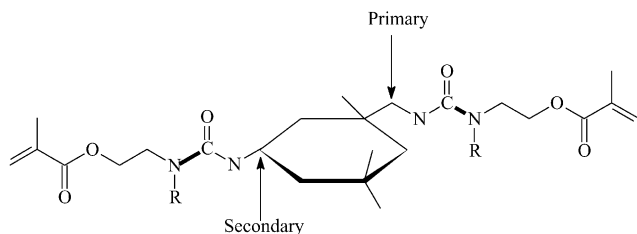


Fig. 1. Generic crosslinker structure used in the modeling experiments.

the user to ‘tune in’ the disassembly temperature based upon their needs. In a publication by Velankar et al., they demonstrated that UV curable methacrylates with sterically hindered urea linkages could be synthesized [25]. Moreover, they showed that the sterically hindered urea linkages were susceptible to attack by basic species. They used this idea to take polymer linkages from one network and sever and simultaneously form linkages with another polymer network to form interpenetrating networks. Based on this reaction, we have studied the controlled thermal degradation of a network comprised of the crosslinker 2-(tert-butylamino)ethyl methacrylate-isophorone diisocyanate-2-(tert-butylamino)ethyl methacrylate (t-BAEM-IPDI-t-BAEM) [Fig. 1, where  $R = -C(CH_3)_3$ ]. This crosslinker had two sterically hindered urea linkages incorporated within it and we showed that we could control the disassembly temperature by careful selection of the amine or alcohol severing agents (herein referred to as basic severing agents) based on the severing agent’s steric and basic properties. These severing agents were nonreactive diluents added to the prepolymer in equal molar quantities to the sterically hindered urea linkages. In addition to the crosslinker and the severing agent, a photoinitiator, and isobornyl methacrylate, a reactive diluent, were added to the prepolymer [26]. Fig. 2 shows the decrosslinking behavior as a function of temperature determined by extractable content of the t-BAEM-IPDI-t-BAEM system when exposed to the severing agents. The data suggests that basic strength followed by steric hindrance of the cleaving species determined the disassembly temperature. Moreover, when

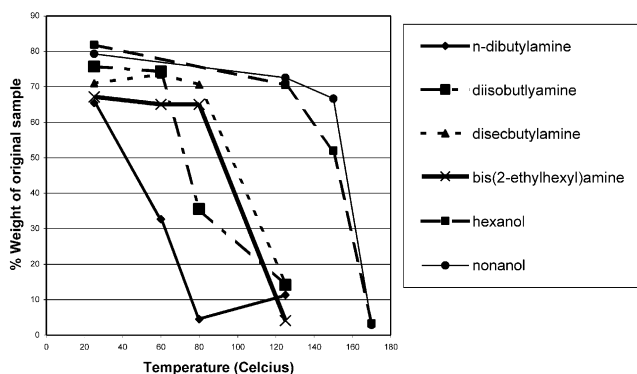


Fig. 2. Decrosslinking behavior for 2-(tert-butylamino)ethyl methacrylate-isophorone diisocyanate-2-(tert-butylamino)ethyl methacrylate when exposed to various bases as a function of temperature.

Table 1

Disassembly temperature behavior for 2-(tert-butylamino)ethyl methacrylate-isophorone diisocyanate-2-(tert-butylamino)ethyl methacrylate when exposed to various bases

Cleaving species	Temperature of 50% disassembly (Celsius)
<i>n</i> -dibutylamine	60
di-isobutylamine	79
bis(2-ethylhexyl)amine	98
di-secbutylamine	108
Hexanol	155
Nonanol	159

non-basic controls were used, the network showed no degradation. Table 1 gives the network disassembly temperature, which for this study is defined as the temperature where 50% of the network has been degraded as determined by extractable content.

The purpose of the work presented here was twofold. Firstly, the reaction to form t-BAEM-IPDI-t-BAEM involves the reaction of an isocyanate and a methacrylic amine (t-BAEM). However, it is not possible to study all possible reworkable structures due to the Michael-type addition reaction that causes amines to react with (meth)acrylates [27]. The t-BAEM molecule is stable because the steric hindrance of the *t*-butyl group attached to the amine renders it stable in the presence of the methacrylate. One can use computational chemistry to assemble molecules and study them theoretically to gain further insight without this limitation. It is claimed by both this team of researchers and also Velankar et al. that reworkability is a function of the steric hindrance imposed by the presence of the *t*-butyl group upon the adjacent urea linkage. To study this idea, a series of molecules was modeled computationally that resembled the t-BAEM-IPDI-t-BAEM molecule and their equilibrium geometry was determined. This family of molecules allowed a comparative study of the effect of changing the *t*-butyl side group to both less and more sterically demanding groups. Based on the results one can determine how changing the R group affects the steric hindrance of the adjacent urea linkage. The second aspect of this study is to use computational simulations to predict the rework temperatures without the need to determine them experimentally. Such a predictive model would be useful as a screening tool to determine which severing compounds would give the desired degradation temperature that a particular application would require.

## 2. Experimental

All computational studies were done using Spartan PC Pro Version 1.0. The simulations were done on a Gateway Solo Pentium 2, 366 MHz computer. Typically, the molecule was built and then the energy minimized using molecular mechanics. The semi-empirical method AM1 was used in

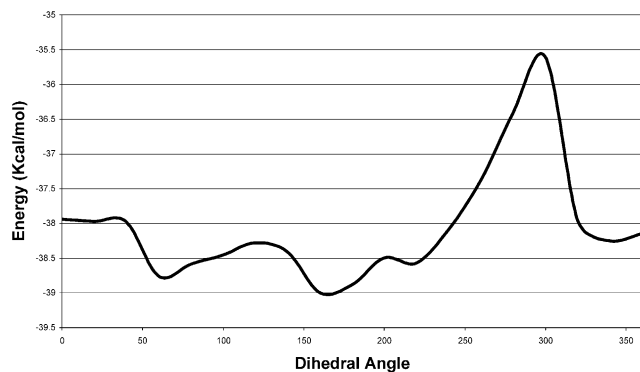


Fig. 3. Energy profile for the dihedral rotation of the model t-Butyl urea compound.

this study because this method provides good results for organic molecules with efficient computational times [28]. Semi-empirical models, like the AM1 Model, reduce computational calculations by using several assumptions and approximations. Since this work is limited to modeling compounds made from carbon, oxygen, nitrogen and hydrogen we will limit our discussion to the approximations used for these elements. The following is assumed in semi-empirical methods. The calculations deal with only the valence electrons with the others remaining fixed, thereby reducing the number of calculations necessary. The calculations for the first row atoms (C, N, O) only deal with the 2s and the three 2p orbitals and hydrogen is represented by the 1s function. Furthermore, semi-empirical methods use the NDDO approximation (Neglect of Diatomic Differential Overlap), which assumes that atomic orbitals on different atomic centers do not overlap, thereby reducing the number of electron–electron interactions, hence reducing the overall calculation. Finally, to further reduce the calculation, additional parameterizations are used from experimental data such as equilibrium geometries, heats of formation, dipole moments etc. Different semi-empirical methods, i.e. PM3, use the same approximations for the calculation but use different experimental parameterization data to simplify the calculation [28].

The rotational energy profile described was done using the following procedure. The molecule was built in an eclipsed formation and the dihedral angle was held fixed. The molecule was minimized with molecular mechanics followed by an AM1 equilibrium geometry optimization. The selected dihedral angle was then rotated in twenty-degree increments and the overall equilibrium geometry/energy was determined while this angle was held fixed. The angle was then rotated another twenty degrees and the equilibrium geometry/energy was again determined. This procedure was repeated until the dihedral angle was rotated the full 360°. The energy at each dihedral angle was then tabulated.

The equilibrium bond distances and the heats of formation were determined by building the specific molecule as

described in Section 3. The dihedral angle was then set to the minimum angle as determined by the above procedure but it was allowed to rotate as needed. The molecule was then minimized using molecular mechanics followed by an equilibrium geometry AM1 calculation. Upon completion of the calculation, the relevant bond distances and the heats of formation were calculated. From the heats of formation, the heats of the reaction were determined as described in Section 3.2.

### 3. Results and discussion

#### 3.1. Comparative study of the change in R groups versus C–N, the bond length in the urea linkage

Velankar et al. and this team of researchers contend that the decrosslinking is a function of the steric hindrance imposed by the presence of the t-butyl group upon the adjacent urea linkage. In any system, as local steric hindrance increases, the bond lengths around the site of steric hindrance should also increase. Moreover, a longer bond length also signifies weaker bond strength. Hence, as the steric hindrance imposed by the ‘R’ group increases, the C–N urea bond length should increase (Fig. 1, with the C–N bonds shown in bold), which in turn causes the bond to be weaker and more susceptible to attack and cleavage. To build a family of molecules that resemble the t-BAEM-IPDI-t-BAEM molecule, it was necessary to determine whether the equilibrium geometries generated around the sterically hindered urea linkages were the global minima and not a local minima. Two separate experiments were needed to generate the equilibrium geometries with the global minima of the sterically hindered urea linkage.

The first experiment involved determining the global rotational minima of a model compound with a sterically hindered urea linkage in it. To find the global minima,  $\text{H}_3\text{C}-\text{N}(\text{H})-\text{C}(\text{O})-\text{N}(\text{C}(\text{CH}_3)_3)(\text{CH}_3)$  was built as the model compound. This model compound possesses the sterically hindered urea linkage. The dihedral angle between the four atoms (highlighted in bold) was rotated to determine the true rotation minima of the sterically hindered urea system. Fig. 3 shows graphically the results of the simulation. The optimal angle is approximately 160° in a clockwise direction from an initially eclipsed formation.

The second experiment involved determining the equilibrium geometries having found an approximation for the rotational minima. The family of t-BAEM-IPDI-t-BAEM structures was built using the template structure in Fig. 1, and by changing the ‘R’ group to various organic groups. The molecules’ equilibrium geometry/energy were determined using the semi-empirical AM1 method. It is noted that in this family of compounds, two types of sterically hindered urea linkages exist in the structure. One linkage has a secondary alpha carbon and the other has a primary alpha carbon (Fig. 1). The dihedral angles of the primary

Table 2  
C–N bond lengths versus volume of side group

Molecule	Volume (Å <sup>3</sup> )	Primary C–N length (Å)	Secondary C–N length (Å)	Mean bond length (Å)
Naphthalenyl	174.830	1.422	1.430	1.426
Cyclopentyl	122.020	1.433	1.412	1.423
<b>t-Butyl</b>	<b>114.740</b>	<b>1.418</b>	<b>1.428</b>	<b>1.423</b>
Benzyl	121.190	1.418	1.418	1.418
Methyl	53.200	1.421	1.412	1.417
Cyclopropyl	85.430	1.418	1.410	1.414
Propyl	95.040	1.413	1.413	1.413
Ethyl	74.050	1.413	1.412	1.413
Cyclohexyl	140.850	1.410	1.413	1.412
Cyclobutyl	103.870	1.412	1.412	1.412
2-Methyl-propyl	114.700	1.414	1.410	1.412
Neopentyl	134.110	1.412	1.410	1.411
Isopropyl	94.610	1.410	1.410	1.410
Hydrogen	31.660	1.415	1.401	1.408

and secondary linkages were initially set at the angle determined from the above rotational experiment, but allowed to rotate from this initial angle to allow the simulation to make adjustments as needed from initial global minima angle determination because of the change in structure from the model compound in the first experiment, a t-BAEM-IPDI-t-BAEM type structure. Both the primary and secondary C–N bond lengths were determined from the simulation. A measure of the size of the side group was also determined. Each of the R groups was built in the simulator and an amino group (–NH<sub>2</sub>) was added where the R group would normally be attached to the rest of the structure (e.g. for R = H, H–NH<sub>2</sub> was used). Each of these side group structures was minimized and their equilibrium geometries and volume (Å<sup>3</sup>) were determined. Table 2 describes the C–N bond length of both the primary and secondary urea linkages. The table was organized in terms of decreasing bond length. If several molecules existed with the same bond length then the side group volume was used as a basis to organize these structures, with the molecule with the largest side group being placed in the table first.

Table 2 suggests which R groups will result in potential molecules with higher and lower degradation temperatures than the t-butyl group derivative. Therefore, based on the data and the experimentally determined behavior of the t-butyl system, one can draw some conclusions. The primary and secondary bond lengths were found to be different, as shown in Table 2. As a method of comparing the various structures we used the mean bond length of the primary and secondary bonds. The mean bond length for the t-butyl derivative is 1.423 Å. Any derivative that has a bond length longer than this length will degrade at a lower temperature with the same severing agents. The naphthalenyl derivative has a bond length of 1.426 Å. Therefore, using the same severing agents this material is expected to decrosslink at a lower temperature. The cyclopentyl derivative has a bond

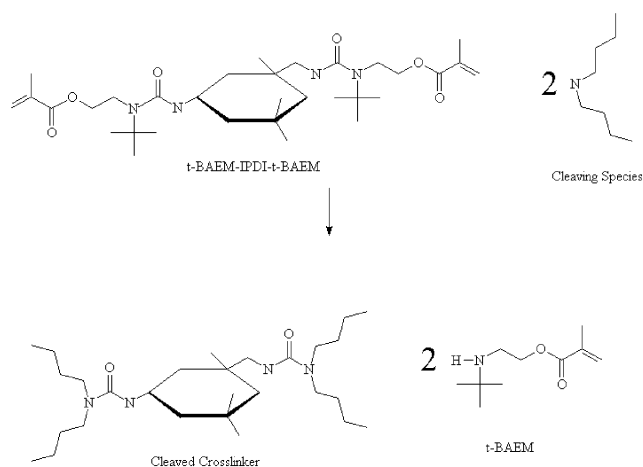


Fig. 4. Severing reaction of t-BAEM-IPDI-t-BAEM that was modelled computationally.

length of 1.4225 Å, therefore, it is predicted to behave in a similar manner to the t-butyl compound. The benzyl compound would be next in the series with a mean bond length of 1.418 Å. This compound would be less reactive than the t-butyl derivative; hence it would show higher rework temperatures for the same severing agents. This procedure can be repeated for all the compounds in the family but certainly the simulations give a likely reactivity order that can aid in selecting other derivatives that might give degradation temperatures one might be interested in, hence providing another method to ‘tune in’ a particular rework temperature.

### 3.2. A predictive decrosslinking temperature model based on simulated heat of reaction data

From the experimental data presented in the introduction, one can determine the reactivity order of any set of severing agents (Table 1). However, the other objective of this work was to determine if the reactivity order could be predicted by theory and to see if a model could be developed. As stated in the introduction, the decrosslinking temperature was a function of the basic strength of the severing agent, but further control could be achieved by its steric hindrance. Since several amines were used in the experimental study to test this steric hindrance theory it is possible to develop a model based on the data generated. To quantify the nature of the steric hindrance of the amines: *n*-dibutylamine, di-isobutylamine, di-secbutylamine and bis(2-ethylhexyl)amine, computation calculations were done to determine the length of the C–N bond in the above amines as a measure of steric hindrance. For *n*-dibutylamine, di-isobutylamine, di-secbutylamine and bis(2-ethylhexyl)amine, the C–N bond lengths were 1.487, 1.492, 1.495 and 1.485 Å, respectively. Therefore, based on the calculations the following reactivity pattern is expected (with decreasing reactivity from left to right): bis(2-ethylhexyl)amine, *n*-dibutylamine, di-isobutylamine, and di-secbutylamine. This is not in agreement with

Table 3  
Computation calculations for  $\Delta H_f^0$  and  $\Delta H^0$  for severing of t-BAEM-IPDI-t-BAEM with various amine agents

Cleaving species	<i>n</i> -Dibutylamine	Di-isobutylamine	Bis(2-ethylhexyl)amine	Di-secbutylamine
Heat of formation (kcal/mol)				
Cleaving species	−45.058	−41.238	−90.127	−37.23
t-BAEM-IPDI-t-BAEM	−242.306	−242.306	−242.306	−242.306
t-BAEM	−88.179	−88.179	−88.179	−88.179
Cleaved crosslinker	−165.53	−156.199	−252.263	−141.262
Heat of reaction (kcal/mol) ( $\Delta H^0$ )	−9.466	−7.775	−6.061	−0.854

Table 4  
Cleaving amine experimental and computational data

Cleaving amine	Temperature of 50% disassembly (°C)	Heat of reaction (kcal/mol) ( $\Delta H^0$ )
<i>n</i> -Dibutylamine	60	−9.466
Di-isobutylamine	79	−7.775
Bis(2-ethylhexyl)amine	98	−6.061
Di-secbutylamine	108	−0.854

experimental data, in which the reactivity order is (from most to least reactive): *n*-dibutylamine, di-isobutylamine, bis(2-ethylhexyl)amine and di-secbutylamine. Therefore, some other model must be generated to predict the reactivity order. Essentially, the severing reaction can be thought of as the reaction depicted in Fig. 4 [26], where, in this case, the severing agent is *n*-dibutylamine. Computational chemistry can readily be used to generate the heat of formation, or standard enthalpy of formation ( $\Delta H_f^0$ ), for each individual species involved in the reaction. Modeling also gives consideration to the steric effects and the lowest energy geometry the molecules must adapt to. From the heats of formation for each of the individual compounds in Fig. 4, one can determine  $\Delta H^0$  for the reaction by the equation  $\Delta H^0 = \sum n\Delta H_f^0(\text{products}) - \sum m\Delta H_f^0(\text{reactants})$ . The  $\Delta H_f^0$  was calculated for each cleaving agent (in the case of Fig. 4, *n*-dibutylamine), t-BAEM-IPDI-t-BAEM, each unique crosslinker product that was the result of the

severing of t-BAEM-IPDI-t-BAEM (in the case of Fig. 4, *n*-dibutylamine-IPDI-*n*-dibutylamine), and the t-BAEM. The results of the  $\Delta H_f^0$  calculations for the amine cleaving agents and the subsequent  $\Delta H^0$  for the reactions are provided in Table 3 (the values generated for the cleaving agent and the t-BAEM were multiplied by two since two moles are involved in the reaction). One can see that the  $\Delta H^0$  calculations accurately predict the reactivity order with the more negative values of  $\Delta H^0$  representing the more reactive amines.

Table 4 presents the amine degradation temperatures given in the introduction and the heats of reaction determined computationally for each amine severing agent from Table 3. Fig. 5 depicts the disassembly temperatures versus the heats of reaction presented in Table 4. Fig. 5 combines the theoretical and the experimental data and shows good agreement between the two sets of data. Moreover, a linear relationship can be seen between the two sets of data:  $\Delta H^0 = 0.159 \times (\text{Temperature of 50\% disassembly}) - 19.751$ . This is significant because it indicates that one can use  $\Delta H^0$  simulations to determine the decrosslinking temperature with any series of amines. This can be extremely useful in the selection of an amine to cause disassembly at a particular rework temperature without the need for experiment. The relationship also suggests that when using amines in this system, the maximum decrosslinking temperature occurs when  $\Delta H^0 = 0$  or at 124 °C. The entropic term is expected to be of equal magnitude in all these calculations since the network degradation method is the same i.e. a crosslinker with two sterically hindered urea linkages present on it being severed by two equivalents of an amine severing agent. Therefore, the entropy contribution is taken into account in the derived relationship because its value is present in the real experimental data, and is used in determination of the model.<sup>1</sup>

Table 5 presents the  $\Delta H^0$  results using the alcohol cleaving agents. One can see that the two alcohols are equally reactive as determined computationally, which is in agreement with experiment. However, it can be seen that based on the computational results, the alcohols have

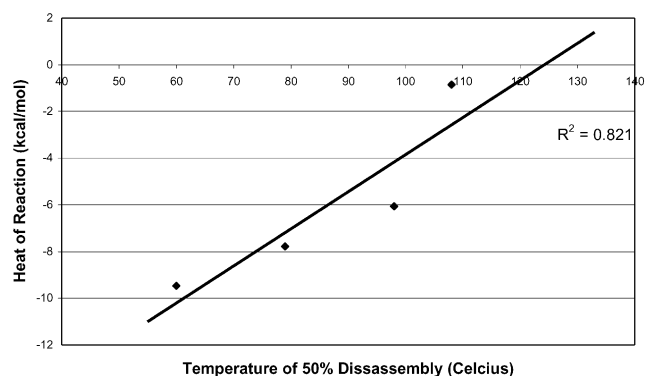


Fig. 5. Disassembly temperature versus the heat of reaction.

<sup>1</sup> The entropic contribution is found to be more important *inter*-system and *intra*-system. This will be the focus of future work.

Table 5

Computation calculations for  $\Delta H_f^0$  and  $\Delta H^0$  for severing of t-BAEM-IPDI-t-BAEM with two alcohol severing agents

Cleaving species	Hexanol	Nonanol
Heat of formation (kcal/mol)		
Cleaving species	−91.644	−112.183
t-BAEM-IPDI-t-BAEM	−242.306	−242.306
t-BAEM	−88.179	−88.179
Cleaved crosslinker	−266.247	−307.326
Heat of reaction (kcal/mol)	−17.011	−17.012

more negative  $\Delta H^0$  values than the amines. This suggests that the alcohol reaction should occur more readily than any amines, hence, have lower rework temperatures. This statement seems to contradict the experimental data. However, this does not provide any conflicting results because the computational calculations only focus on the energy difference between the reactants and the products without any consideration for the potential energy profile. The computational calculations, as modeled, fail to consider the transition state energy. If one considers the transition states, then depending on whether an amine or an alcohol attacks the urea linkage, one of two transition states is possible (Fig. 6). Looking at the urea carbon that is attacked during the decrosslinking process, prior to the attack by the decrosslinking agent, it has two nitrogens and one oxygen attached to it. In short, this carbon is very electron deficient. Therefore, when attacked by the amine, which is more basic than the alcohol, the amine will better stabilize the transition state. Hence, the transition state energy when using amines will be lower compared to the attack by alcohols. In either case, since the reaction is not spontaneous at room temperature, but requires elevated temperatures and since  $\Delta G = \Delta H - T\Delta S$ , this implies that the entropy term ( $-T\Delta S$ ) is also negative and, as the temperature rises, it becomes larger. Moreover, at some point the entropy term is large enough to overcome the transition state energy barrier causing the decrosslinking reaction to occur. This explains why the amines have lower decrosslinking reactions compared with the alcohols. Therefore, the computational calculations are not erroneous but rather fail to take into account all of the specifics of the reaction pathway. However, the simulations indicate that they can be a good predictive tool provided that they only consider the same type of cleaving agents.

#### 4. Conclusions

The computational simulations described herein provide further insight into the disassembly of molecules with sterically hindered urea linkages. The molecular disassembly hypothesis is based on the idea that the presence of the t-butyl group strains the urea linkage making it susceptible to

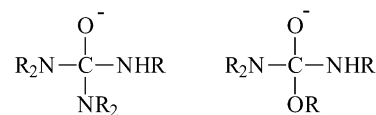


Fig. 6. Transition states for the decrosslinking reaction.

cleavage by a base [25]. Using computational chemistry, it was possible to study a family of reworkable structures without the limitations imposed by ‘real world’ synthesis [26]. Using these methods other likely candidates that could be reworkable, based on the calculated steric strains as a function of the R group, can be determined. Moreover, the study also provides some insight into the relative ordering of the family of structures against one another. While the Michael addition reaction provides hurdles to the synthesis of these other molecules, it does not make their synthesis impossible. Therefore, using the information generated in this study, it would be possible to generate structures that would allow rework and provide another way to further control the degradation temperature.

The second part of this work focused on using the data generated to develop a model that would predict the decrosslinking temperature in the t-BAEM-IPDI-t-BAEM system. A computational model that calculated the heat of reaction of a similar type of severing agent was found to accurately predict the reactivity order. Moreover, when this data was plotted against the experimental data, a linear relationship emerged. Based on this relationship, it was possible to determine the upper limit for attack of the t-BAEM-IPDI-t-BAEM system with amine severing agents. Furthermore, using the relationship it would be possible to get an estimate of the rework temperature for any amine severing agent. Therefore, if practitioners desire a particular rework temperature they could select likely amine candidates based on the calculations prior to experimentation.

The bond length calculations were used to determine the expected behavior of changing the R group on the crosslinker structure. The enthalpy method focuses on the nature of the severing agent. The first method focuses on changes that would allow control of the disassembly temperature on the crosslinker structure while the second focus on control through selection of the severing agent. Only when both perspectives are considered can one get a complete understanding of the two primary factors that control the rework temperature since they are both complementary to one another.

In conclusion, computational methods have been shown to provide much insight into the controlled degradation of the t-BAEM-IPDI-t-BAEM polymer networks. The data generated in this study allows a firmer understanding of the factors that control the network degradation and, more importantly, allows users to manipulate the information to provide for the particular rework temperatures they desire for their applications.

## References

- [1] Griffith JR. *Org Coat Plast* 1978;39:209.
- [2] Lau JH. *Flip chip technologies*. New York: McGraw Hill, 1996.
- [3] Lau JH. *Low cost flip chip technologies for DCA, WLCSP, and PBGA assemblies*. New York: McGraw Hill, 2000.
- [4] Hoffmeyer MK. US Patent 5,757,073.
- [5] Layman PL. *Chem Engng News* 1993;71:11.
- [6] Manzione LT. *Plastic packaging of microelectronic devices*. New York: Van Nostrand Reinhold, 1990.
- [7] Lau JH. *Chip on board technologies for multichip modules*. New York: Van Nostrand Reinhold, 1994.
- [8] Stevens JJ. *Epoxy resin technology*. New York: Interscience Publishers, 1968.
- [9] Buchwalter SL, Kosbar LL. *J Poly Sci: Part A: Poly Chem* 1996;34:249.
- [10] Afzali-Ardakani A, Buchwalter SL, Gelorme JD, Kosbar LL, Pompeo FL. US Patent 5,512,613.
- [11] Afzali-Ardakani A, Buchwalter SL, Gelorme JD, Kosbar LL, Newman BH, Pompeo FL. US Patent 5,560,934.
- [12] Yang S, Chen J-S, Körner H, Breiner T, Ober CK, Poliks MD. *Chem Mater* 1998;10:1475.
- [13] Yang S, Chen J-S, Körner H, Breiner T, Ober CK. *Poly Prepr* 1997;38:440.
- [14] Wang L, Wong CP. *J Poly Sci: Part A: Poly Chem* 1999;37:2991.
- [15] Wong CP, Wang L, Shi S-H. *Mater Res Innovat* 1999;2:232.
- [16] Iyer SR, Land S, Wong PK. US Patent 5,726,391.
- [17] Iyer SR, Land S, Wong PK. US Patent 5,760,337.
- [18] Tesoro GC, Sastri V. *J Appl Poly Sci* 1990;39:1425.
- [19] Tesoro GC, Sastri V. *J Appl Poly Sci* 1990;39:1439.
- [20] Hall JB, Hogerton PB, Pugol JM. US Patent 5,457,149.
- [21] Sachdev KG, Berger M, Chace MS. US Patent 5,700,581.
- [22] Grube W, Khandros IY. US Patent 5,086,558.
- [23] Call AJ, Buchwalter SL, Iruvanti S, Jasne SJ, Pompeo FL, Zacco PA, Moreau WM. US Patent 5,659,203.
- [24] Call AJ, Buchwalter SL, Iruvanti S, Jasne SJ, Pompeo FL, Zacco PA, Moreau WM. US Patent 5,930,597.
- [25] Velankar S, Pazos J, Cooper SL. *J Appl Poly Sci* 1996;62:1361.
- [26] Malik J, Goldsleger BA, Clarson SJ. *J Appl Poly Sci*, in press.
- [27] Lee C-L, Lutz MA. US Patent 4,697,026.
- [28] Hehre WJ, Yu J, Klunzinger PE, Lou L. *A brief guide to molecular mechanics and quantum chemical calculations*. California: Wavefunction Inc, 1998.